Journal of Metals, Materials and Minerals, 37(1), e2683, 2027

Tailoring energy storage properties of epoxy composites using ferroelectric, anti-ferroelectric particles and hybrid ceramic fillers

Apinya SASIPONGPAN[1], Nakulkarn RERNGROEN[1] and Wanwilai VITTAYAKORN[1,*]

[1] *Department of Nanoscience and Nanotechnology, School of Integrated Innovative Technology, King Mongkut's Institute of Technology Ladkrabang, 1 Chalongkrung Road, Ladkrabang, Bangkok 10520 Thailand*

***Corresponding author e-mail**: wanwilai.vi@kmitl.ac.th

Received date:
24 March 2026
Revised date:
14 August 2026
Accepted date:
29 September 2026

Keywords:
Ferroelectric;
Antiferroelectric;
Epoxy-based composites;
Energy storage performance

Abstract

Epoxy-based dielectric composites reinforced with ferroelectric $BaTiO_3$ and antiferroelectric $AgNbO_3$ were fabricated and comprehensively evaluated to investigate the influence of filler type and composition on dielectric and energy storage performance. Structural, spectroscopic and microstructural analyses confirmed the successful incorporation of the ceramic fillers within the epoxy matrix. $BaTiO_3$/epoxy composites exhibited markedly enhanced dielectric permittivity and polarization, resulting in a maximum recoverable energy density of 134.4 $\mu J \cdot cm^{-3}$, albeit with moderate charge-discharge efficiency due to hysteresis-induced energy loss. In contrast, $AgNbO_3$/epoxy composites displayed lower permittivity but significantly reduced dielectric loss and excellent efficiency, reaching up to 96.7%, owing to low remanent polarization and a highly reversible dielectric response. Building on these complementary characteristics, hybrid $BaTiO_3$-$AgNbO_3$/epoxy composites were developed and found to provide complementary improvements in dielectric and energy-storage performance. The optimal hybrid formulation (15 wt% $BaTiO_3$/30 wt% $AgNbO_3$) achieved the highest recoverable energy density of 155.8 $\mu J \cdot cm^{-3}$, while the equimolar hybrid (22.5/22.5) provided exceptional efficiency of 99.06% with minimal energy loss. These enhancements arise from the complementary dielectric responses of the two ceramic fillers together with polymer-ceramic interfacial effects. The results demonstrate that combining ferroelectric and antiferroelectric fillers offers a powerful strategy for tailoring the dielectric response and optimizing energy storage performance in polymer-based composites.

1. Introduction

The increasing demand for high-performance energy storage systems has intensified research on advanced dielectric materials that offer high energy density, excellent efficiency, and operational reliability [1]. Polymer-based dielectrics, particularly epoxy resins, have emerged as promising candidates due to their high breakdown strength, low density, mechanical robustness, and ease of processing. However, the inherently low dielectric constant and limited polarization capability of epoxy restrict its energy storage potential. To overcome these limitations, functional ceramic fillers are widely incorporated into polymer matrices to enhance permittivity, interfacial polarization, and electrostatic energy storage behavior [2,3].

Among such fillers, ferroelectric (FE) and antiferroelectric (AFE) ceramics, such as barium titanate ($BaTiO_3$), lead zirconate titanate (PZT), and lead zirconate ($PbZrO_3$), have been extensively investigated because of their high dielectric permittivity, tunable phase transitions, and field-responsive polarization characteristics [4–6]. Ferroelectric materials exhibit spontaneous polarization that can be aligned under an external electric field, thereby significantly increasing stored electrostatic energy. However, strong hysteresis behavior often results in high energy dissipation and reduced charge-discharge efficiency [5,7]. By contrast, antiferroelectric ceramics undergo a reversible field-induced transition from an antipolar to a polar state, enabling high recoverable energy density with minimal remanent polarization and substantially lower energy loss. These complementary polarization mechanisms make both FE and AFE ceramics attractive for tailoring dielectric performance in polymer-based energy storage devices.

In this study, $BaTiO_3$ and $AgNbO_3$ were selected as representative lead-free FE and AFE fillers, respectively, owing to their environmental safety and favorable dielectric characteristics. $BaTiO_3$ possesses a high dielectric constant (~1000 to 5000), strong spontaneous polarization, and excellent chemical stability, which facilitate efficient interfacial polarization and charge accumulation within epoxy matrices. $AgNbO_3$, on the other hand, offers a distinctive field-induced AFE-FE phase transition, high recoverable energy density, low remanent polarization, and good thermal and cycling stability, all desirable features for high-efficiency polymer capacitors [8–9]. Previous studies on $BaTiO_3$/epoxy composites have demonstrated significant improvements in permittivity and energy density, particularly when particle connectivity is enhanced or hierarchical structures are introduced [10–13]. Meanwhile, $AgNbO_3$ fillers have shown promise in epoxy and other polymeric matrices, particularly when surface-modified to improve dispersion and suppress space-charge accumulation, leading to improved dielectric reliability and breakdown strength [14]. Although the energy-storage behavior of $AgNbO_3$ has been widely studied in bulk ceramics and PVDF-based

polymers [15,16], its performance within epoxy matrices remains comparatively underexplored.

Despite the progress made with FE- or AFE-filled polymer composites, direct comparative studies evaluating $BaTiO_3$ and $AgNbO_3$ under identical processing and testing conditions are limited. Furthermore, hybrid dielectric systems, where ferroelectric and antiferroelectric fillers are combined within a single polymer matrix, offer a promising yet underinvestigated strategy for simultaneously enhancing permittivity, suppressing dielectric loss, and improving charge-discharge efficiency. The coexistence of FE and AFE phases has the potential to generate synergistic effects through interfacial heterogeneity, improved filler dispersion, complementary polarization dynamics, and modified local electric field distributions [17,18]. However, systematic studies on the dielectric and energy storage characteristics of $BaTiO_3$-$AgNbO_3$ hybrid epoxy composites are scarce.

Therefore, the present study aims to (i) fabricate and characterize epoxy composites reinforced individually with $BaTiO_3$ and $AgNbO_3$ fillers, (ii) compare their dielectric and energy-storage performances under consistent processing conditions, and (iii) investigate hybrid $BaTiO_3$-$AgNbO_3$/epoxy systems to assess potential synergistic enhancements arising from the interaction between FE and AFE fillers. The insights gained from this comparative and hybrid analysis are expected to provide a deeper understanding of polarization mechanisms in polymer dielectrics and guide the rational design of next-generation epoxy-based materials for high-energy-density and high-efficiency capacitive applications.

2. Experimental procedures

2.1 Materials

Epoxy resin (bisphenol A-epichlorohydrin polymer) and hardener [poly(oxy(methyl-1,2-ethanediyl)), α-hydro-ω-(2-aminomethylethoxy)-ether with 2-ethyl-2-hydroxymethyl-1,3-propanediol (3:1)], supplied by Buehler (EPOXICURETM 2), were used as the polymer matrix. Ferroelectric barium titanate ($BaTiO_3$) nanopowder (99.95% purity, ~50 nm particle size) was purchased from Inframat® Advanced MaterialsTM, while antiferroelectric silver niobate ($AgNbO_3$) nanopowder was synthesized in-house from Ag_2O (≥99%, Sigma Aldrich) and Nb2O5 (≥99.9%, Inframat® Advanced MaterialsTM).

2.2 Synthesis of $AgNbO_3$ powder

$AgNbO_3$ powder was synthesized via a conventional solid-state reaction route according to the following reaction:

$$Ag_2O_{(s)} + Nb_2O_{5(s)} \rightarrow 2AgNbO_{3(s)}$$

Stoichiometric quantities of Ag_2O and Nb_2O_5 were weighed, mixed, and vibratory ball-milled with alumina media in ethanol for 2 h. The slurry was dried, ground, and calcined at 900°C for 6 h in air with heating and cooling rates of 5°C·min^{-1}. The formation of phase-pure $AgNbO_3$ was confirmed by X-ray diffraction (XRD). $BaTiO_3$ powder was used as received.

2.3 Fabrication of epoxy-based composites

The epoxy resin and hardener were mixed in a 100:23 (w/w) stoichiometric ratio following a standard casting process and pre-cured at room temperature for 6 h. Ceramic fillers ($BaTiO_3$ or $AgNbO_3$) were incorporated at 40 wt%, 45 wt%, and 50 wt% loadings. Each filler was dispersed in the epoxy resin using magnetic stirring for 30 min at room temperature. The hardener was then added and stirred for an additional 2 min to ensure homogeneity. The mixture was vacuum degassed at ~700 mmHg to remove entrapped air, cast into molds, and cured overnight at room temperature.

In addition, hybrid $BaTiO_3$-$AgNbO_3$/epoxy composites were also fabricated to investigate the combined influence of ferroelectric and antiferroelectric fillers on dielectric and energy storage behavior. The specific hybrid formulations were selected after analyzing the performance trends of the single-filler systems, ensuring that the chosen compositions were representative of the most promising ratios for further evaluation. All hybrid composites were processed using the same mixing, degassing, and curing procedures as the single-filler samples.

2.4 Characterization techniques

All structural, microstructural, dielectric, and energy-storage measurements were performed on pure epoxy, single-filler ($BaTiO_3$ or $AgNbO_3$), and hybrid $BaTiO_3$-$AgNbO_3$ composites to enable direct comparison under identical testing conditions.

2.4.1 Structural and chemical analysis

XRD (Rigaku SmartLab®, Cu Kα radiation) was used to confirm crystalline phases of $BaTiO_3$ and $AgNbO_3$ and to analyze composite structures. Fourier transform infrared (FT-IR) spectroscopy (Spectrum GX, PerkinElmer) was performed to examine chemical composition and matrix-filler interactions. Optical microscopy was used to observe the macroscopic morphology of the composites. Particle size distributions of the $BaTiO_3$ and $AgNbO_3$ powders were evaluated by dynamic light scattering (DLS) using a DelsaTM Nano particle analyzer (Beckman Coulter) with water as the dispersion medium at 25°C.

2.4.2 Microstructural analysis

Fractured cross-sections of composites were examined using scanning electron microscopy (SEM, JEOL Ltd.), and energy-dispersive X-ray spectroscopy (EDX) was used to analyze elemental distribution and filler dispersion.

2.4.3 Electrical and energy storage measurements

Silver paste electrodes were applied to both sides of each sample. Dielectric properties were measured using an LCR meter (HP-4284A, Hewlett-Packard Inc.) over the frequency range 100 Hz to 1 MHz. The dielectric constant (εr) was calculated from measured capacitance and sample dimensions. Polarization-electric field (P-E) hysteresis loops were obtained at room temperature using a ferroelectric tester (RT66A, Radiant Technologies) to determine recoverable energy density and loss energy. Breakdown strength (EBD) and related electrical parameters were also evaluated.

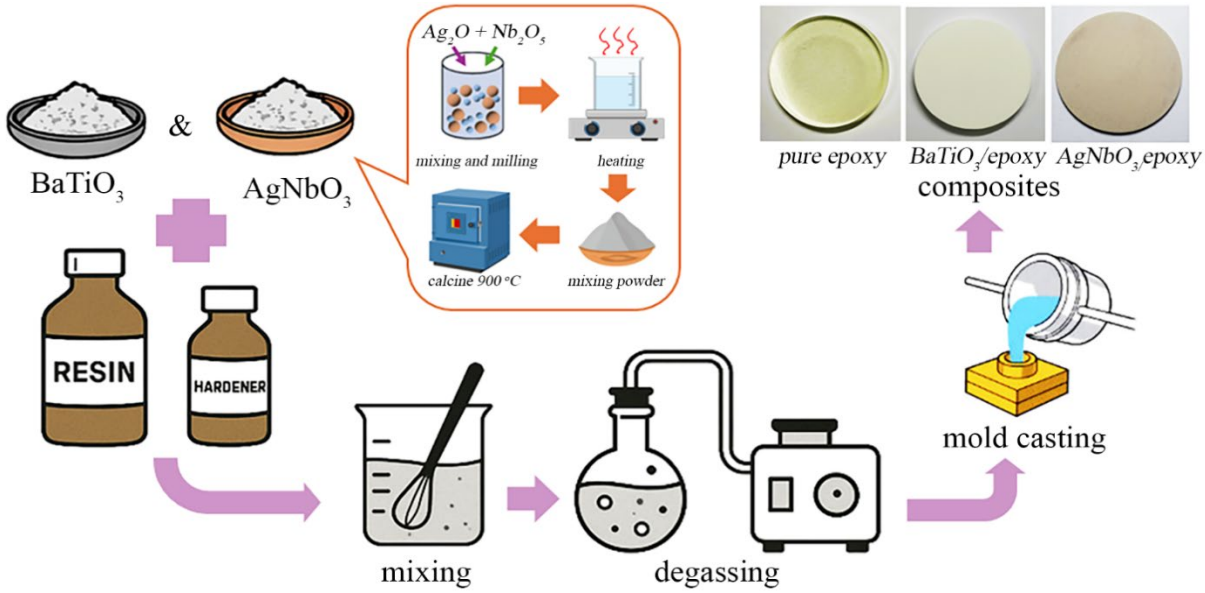


Figure 1. Schematic representation of the fabrication process for epoxy-based composites reinforced with $BaTiO_3$ and $AgNbO_3$ fillers.

3. Results and discussion

3.1 Structural and chemical characterization

Figure 2 (top row) displays the XRD patterns of pure epoxy resin, 50 wt% $BaTiO_3$/epoxy, and 50 wt% $AgNbO_3$/epoxy composites. Pure epoxy exhibits a broad amorphous halo centered at 2θ ~ 20° to 30°, a characteristic feature of its non-crystalline thermoset structure [19]. In contrast, the $BaTiO_3$/epoxy composite shows sharp diffraction peaks consistent with the tetragonal $BaTiO_3$ phase (JCPDS file no. 05-0626) [20], while the $AgNbO_3$/epoxy composite presents distinct reflections corresponding to orthorhombic $AgNbO_3$ (JCPDS file no. 52-0405) [21]. These results confirm that both ceramic fillers preserve their crystalline structures upon incorporation into the epoxy matrix and that no new secondary phases formed during composite fabrication.

Figure 2 (middle row) shows photographic images comparing the visual appearance of the samples. Pure epoxy is transparent with a slight yellow hue, which is typical of cured bisphenol-A-based resins [22]. The $BaTiO_3$/epoxy composite appears opaque white due to strong scattering effects caused by the high refractive index of $BaTiO_3$ particles [23], whereas the $AgNbO_3$/epoxy composite exhibits a beige color consistent with the intrinsic pigmentation of $AgNbO_3$ powder. These observations suggest uniform filler distribution at the macroscopic scale.

The FTIR spectra in Figure 2 (bottom row) further verify the chemical structure of the composites and reveal potential interfacial interactions between the fillers and the polymer matrix. The pure epoxy resin exhibits characteristic absorption bands associated with C–H stretching (~2950 cm^{-1}), aromatic C–C stretching (~1509 cm^{-1}), and symmetrical aromatic C–O stretching (~1030 cm^{-1}) [24]. These bands remain present in both $BaTiO_3$- and $AgNbO_3$- filled composites, although slight peak broadening and reduced intensity are observed, indicating possible matrix-filler interactions [25]. In the $BaTiO_3$/epoxy composite, an additional peak appears at 490 cm^{-1}, corresponding to Ti–O vibration modes typical of $BaTiO_3$ ceramics [26]. Similarly, the $AgNbO_3$/epoxy composite exhibits a distinct peak near ~480 cm^{-1} attributed to Nb–O bending modes [27]. The retention of these characteristic vibrational signatures confirms the successful incorporation of $BaTiO_3$ and $AgNbO_3$ into the epoxy matrix while maintaining their chemical identities. These molecular-level interactions and filler signatures may influence the composites' dielectric response, polarization behavior, and overall energy storage performance.

3.2 Microstructure and filler dispersion

Particle size analysis revealed broad particle size distributions for both ceramic powders. The smaller-size population was centered at approximately 0.76 μm to 0.97 μm for $AgNbO_3$ and 0.62 μm to 1.43 μm for $BaTiO_3$, while larger agglomerated populations extending into the tens-of-micrometers range were also observed. These results indicate the presence of particle agglomeration in both ceramic powders. However, the DLS-derived sizes represent hydrodynamic particle/agglomerate sizes in suspension and therefore should not be interpreted as the primary crystallite or manufacturer-specified particle size. Figure 3 presents the SEM micrograph, EDX spectra, and elemental mapping of the epoxy composite containing 50 wt% $BaTiO_3$. The SEM image reveals densely packed $BaTiO_3$-rich region embedded within the epoxy matrix, with some local particle aggregation [28,29]. Two representative regions were selected for EDX analysis, labeled Spectrum 1 and Spectrum 3. Spectrum 1, obtained from a $BaTiO_3$ particle, shows strong signals for barium (47.94 wt%), titanium (15.47 wt%), and oxygen (11.96 wt%), confirming the ceramic composition. A moderate carbon signal (24.63 wt%) is also detected, which is attributed to contributions from the surrounding epoxy matrix or surface contamination. In contrast, Spectrum 3, corresponding to an epoxy-rich region, exhibits dominant carbon content (73.69 wt%) and oxygen (26.31 wt%) contents with no detectable barium or titanium, clearly confirming the polymer phase. Elemental mapping confirms the spatial distribution of Ba and Ti throughout the analyzed composite region. This ceramic-rich microstructure provides extensive polymer-ceramic interfaces that may contribute to interfacial polarization and enhanced dielectric response [30] although local particle aggregation may promote localized leakage pathways at high filler concentrations [31].

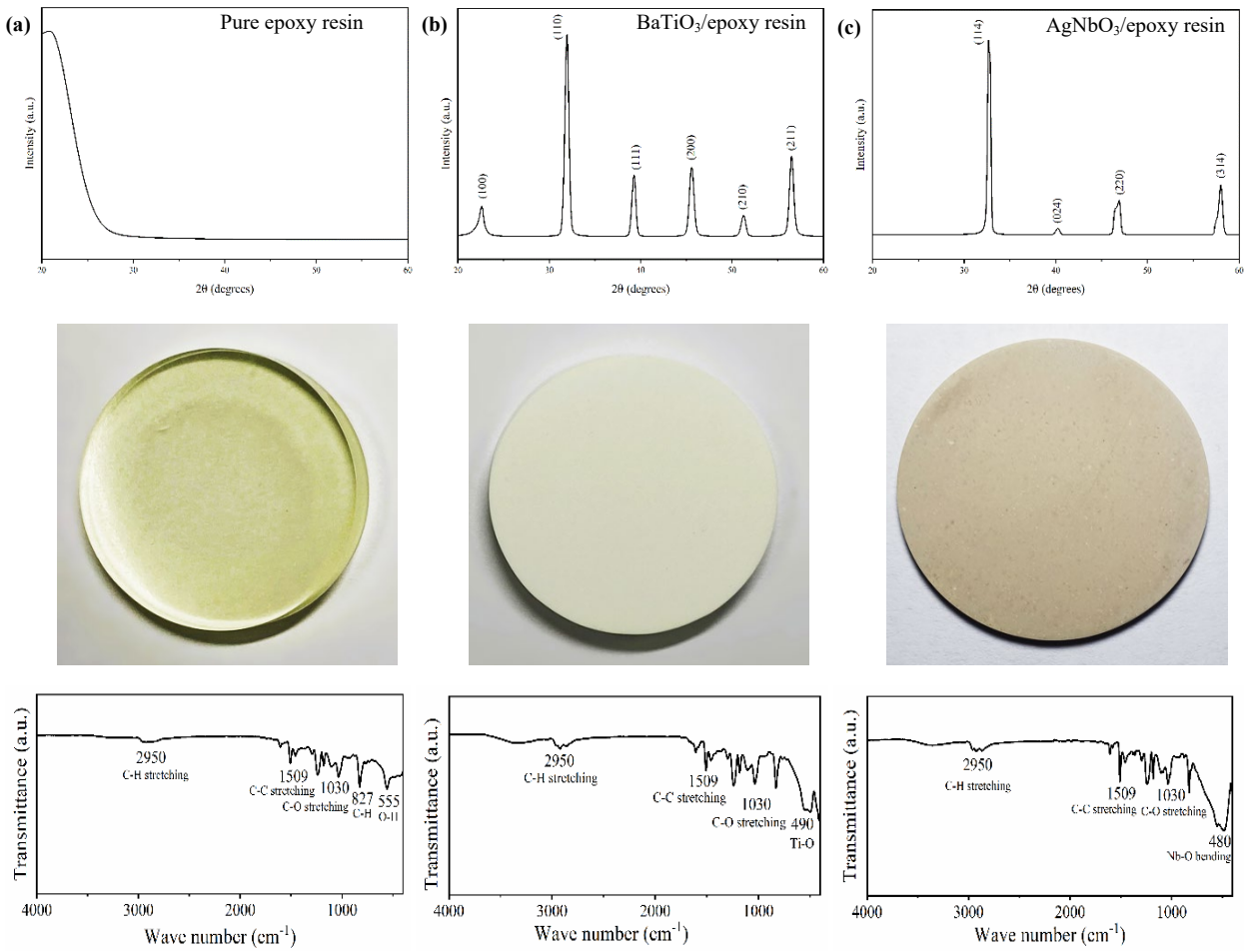


Figure 2. XRD patterns (top row), photographic images (middle row), and FTIR spectra (bottom row) of (a) pure epoxy resin, (b) 50 wt% $BaTiO_3$/epoxy resin composite and (c) 50 wt% $AgNbO_3$/epoxy resin composite.

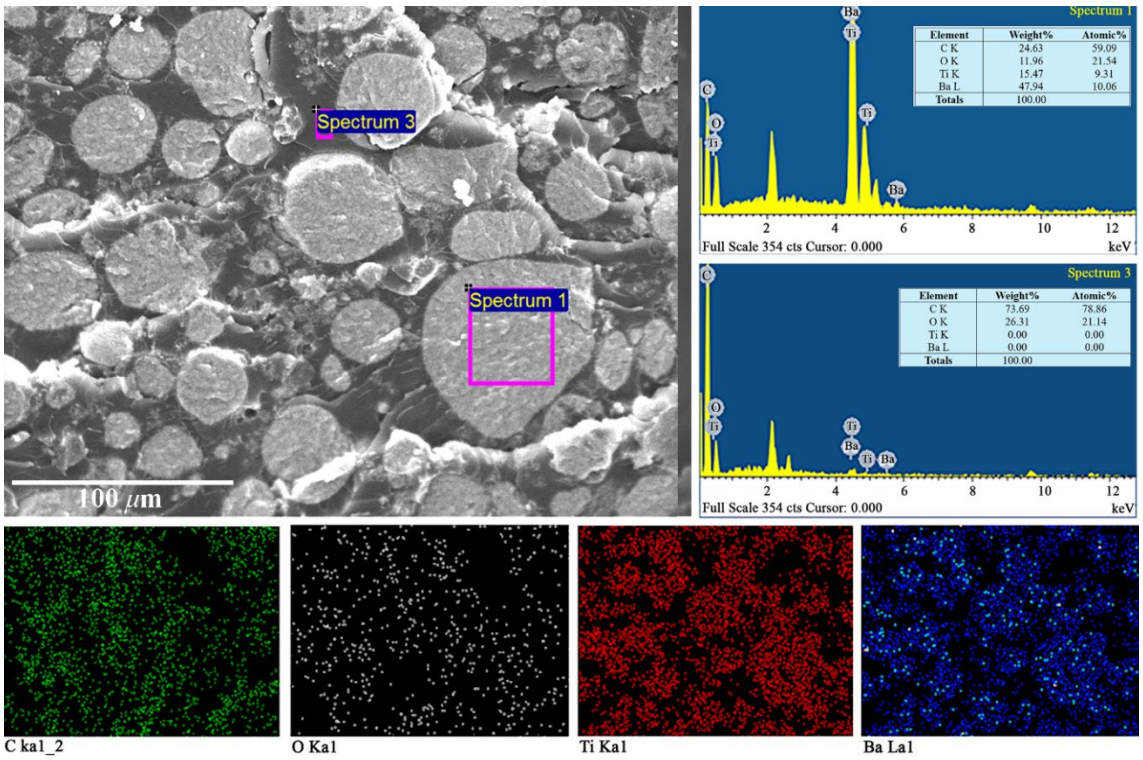


Figure 3. SEM micrograph, EDX analysis and element mapping of epoxy resin filled with 50 wt% $BaTiO_3$ composite.

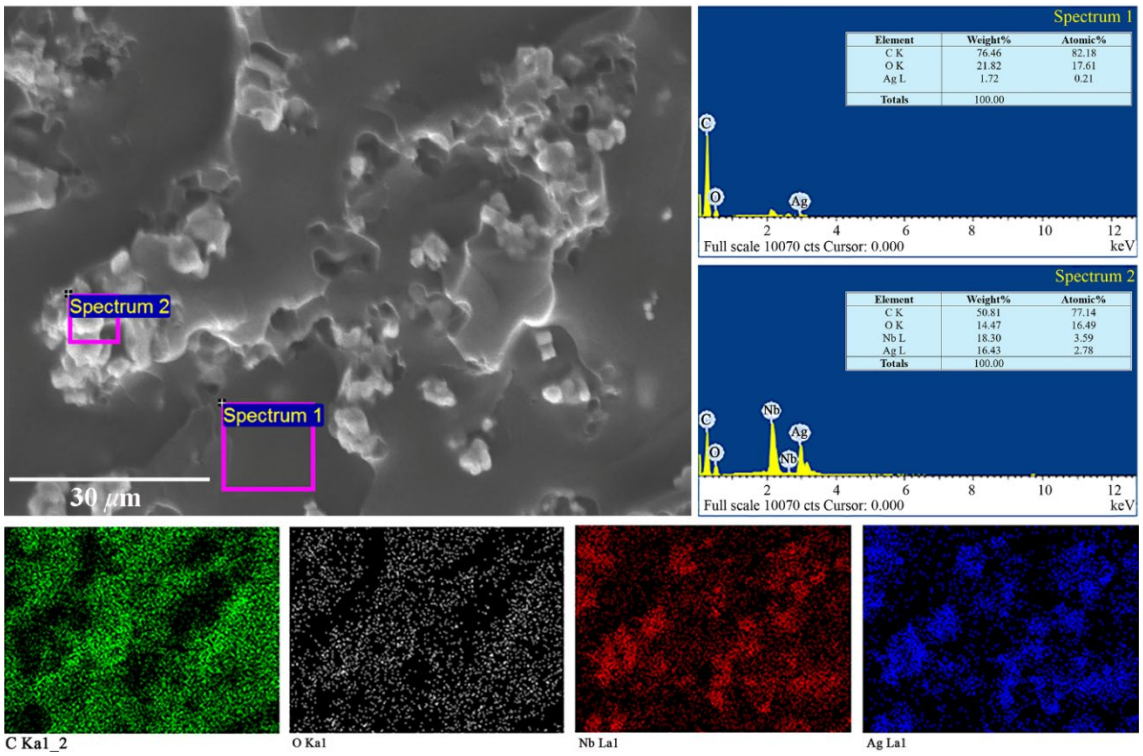


Figure 4. SEM micrograph, EDX analysis and element mapping of epoxy resin filled with 50 wt% $AgNbO_3$ composite.

Figure 4 shows the SEM-EDX and elemental mapping results of the epoxy composite filled with 50 wt% $AgNbO_3$. The $AgNbO_3$ particles exhibit irregular angular morphologies and are distributed throughout the epoxy matrix, with no obvious large interfacial voids observed in the analyzed region [32]. EDX analysis of the ceramic-rich region (Spectrum 2) confirms the presence of Ag, Nb, and O, while the polymer-rich region (Spectrum 1) is dominated by C and O, confirming the distinction between ceramic-rich and polymer-rich regions. The elemental maps of Ag and Nb show well-localized ceramic domains throughout the composite. The observed $AgNbO_3$ distribution and associated polymer-ceramic interfaces may contribute to the effective dielectric response and energy-loss behavior of the composite [33].

Figure 3 and Figure 4 reveal different microstructural characteristics of the $BaTiO_3$/epoxy and $AgNbO_3$/epoxy composites, although a direct comparison of particle size from these images is not appropriate because they were acquired at different magnifications. Together with the particle size analysis, microstructural observations indicate that the dielectric behavior of these composites is influenced not only by the intrinsic dielectric characteristics of the ceramic fillers but also by particle aggregation/agglomeration, filler distribution, and polymer-ceramic interfacial effects [16,34]. These factors may moderate the differences in the effective dielectric response of the $BaTiO_3$/epoxy and $AgNbO_3$/epoxy composites.

3.3 Dielectric properties, dielectric modelling and theoretical analysis

Figure 5 illustrates the frequency-dependent dielectric behavior of epoxy resin-based composites incorporated with ferroelectric $BaTiO_3$ and antiferroelectric $AgNbO_3$ fillers in terms of dielectric constant (ε_r) and dielectric loss (tan δ). As shown in Figure 5(a), pure epoxy resin exhibits a low and nearly frequency-independent dielectric constant of approximately 5 over the measured frequency range of 100 Hz to 1 MHz, reflecting its intrinsically low polarizability. Upon incorporation of ceramic fillers, both $BaTiO_3$- and $AgNbO_3$-filled composites show a pronounced enhancement in ε_r. For all samples, ε_r gradually decreases with increasing frequency, which is characteristic of the diminishing contribution of interfacial polarization at high frequencies [35]. Among the two systems, $BaTiO_3$-filled composites consistently exhibit higher dielectric constants than their $AgNbO_3$-filled counterparts at all filler loadings. This behavior is attributed to the intrinsically high permittivity and strong ferroelectric polarization of $BaTiO_3$. Moreover, increasing the filler content from 40 wt% to 50 wt% further enhances the dielectric response. At higher filler contents, the average interparticle distance is expected to decrease, leading to increased filler-filler interactions and changes in the polymer-ceramic interfacial contribution. At the same time, the increased probability of local particle agglomeration at high filler loadings may affect the dielectric response. Therefore, the filler-content dependence of the dielectric properties reflects the combined effects of increasing ceramic fraction, particle distribution, and interfacial interactions within the epoxy matrix. Figure 5(b) presents the corresponding dielectric loss (tanδ) as a function of frequency. Pure epoxy shows low and relatively constant dielectric loss, indicating minimal energy dissipation. In contrast, the introduction of ceramic fillers leads to increased tanδ, particularly in the low-frequency region (<10 kHz), due to interfacial polarization and space-charge accumulation at the polymer-ceramic interfaces, commonly described by the Maxwell-Wagner-Sillars (MWS) effect [36].

$BaTiO_3$-filled composites exhibit higher dielectric loss than $AgNbO_3$-filled systems, especially at high filler loadings. This behavior is attributed to stronger interfacial polarization, a larger permittivity mismatch between filler and matrix, and the formation of microcapacitor

networks that promote localized leakage pathways [37]. With increasing frequency, all samples exhibit decreasing dielectric loss due to reduced charge carrier mobility and suppressed dipole relaxation [38]. While $BaTiO_3$/epoxy composites provide superior dielectric constants, their relatively higher losses may limit performance in low-dissipation applications. In contrast, $AgNbO_3$/epoxy composites offer a more balanced performance, featuring moderate εr enhancement and lower tan δ across the frequency range, making them more suitable for applications requiring dielectric stability, such as embedded capacitors and insulating layers.

Figure 6 compares the experimental dielectric constant measured at 1 kHz with predictions from classical dielectric mixing models, including the Series, Parallel, Lichtenecker, Maxwell-Garnett, and Jayasundere-Smith models [39–42] for (a) $BaTiO_3$- and (b) $AgNbO_3$-filled composites. For $BaTiO_3$-filled composites (Figure 6(a)), the experimental dielectric constant (•) increases nonlinearly with increasing filler content, particularly beyond 45 wt%, indicating that the dielectric response becomes increasingly sensitive to filler-filler and polymer-ceramic interfacial interactions at higher filler concentrations. The Series and Parallel models define the theoretical lower and upper bounds, respectively, but fail to describe the experimental behavior due to their oversimplified assumptions. The Lichtenecker model slightly overestimates ε_r at higher filler loadings, as it assumes ideal logarithmic mixing without considering interfacial polarization, agglomeration, or filler-filler interactions. The Maxwell-Garnett model underpredicts εr because it is valid only for dilute, non-interacting spherical inclusions. In contrast, the Jayasundere-Smith model shows the closest agreement with experimental data, particularly at high filler concentrations. This model is a modified extension of the Maxwell-Garnett theory that incorporates cooperative interparticle interactions at elevated filler loadings. The effective dielectric constant is expressed as:

$$\varepsilon_C = \frac{\varepsilon_m V_m + \varepsilon_f V_f \left[\frac{3\varepsilon_m}{\varepsilon_f + 2\varepsilon_m}\right]\left[1 + \frac{3V_f(\varepsilon_f - \varepsilon_m)}{\varepsilon_f + 2\varepsilon_m}\right]}{V_m + V_f \left[\frac{3\varepsilon_m}{\varepsilon_f + 2\varepsilon_m}\right]\left[1 + \frac{3V_f(\varepsilon_f - \varepsilon_m)}{\varepsilon_f + 2\varepsilon_m}\right]} \quad (1)$$

where ε_C, εm and ε_f are the dielectric constants of the composite, matrix and filler, respectively, and V_m and V_f are their corresponding volume fractions. The close agreement suggests that interparticle and interfacial interactions contribute to the dielectric response of $BaTiO_3$-filled epoxy composites. However, the effective dielectric behavior is also influenced by microstructural factors, including particle distribution and agglomeration within the epoxy matrix.

For $AgNbO_3$-filled composites (Figure 6(b)), the experimental dielectric constant (•) increases with increasing filler content, with a noticeable increase between 40 wt% and 45 wt%. A similar composition-dependent trend is also observed for the $BaTiO_3$-filled composites. Among the investigated models, the Lichtenecker model provides the closest agreement with the experimental results for the $AgNbO_3$/epoxy composites. This model follows a logarithmic mixing rule:

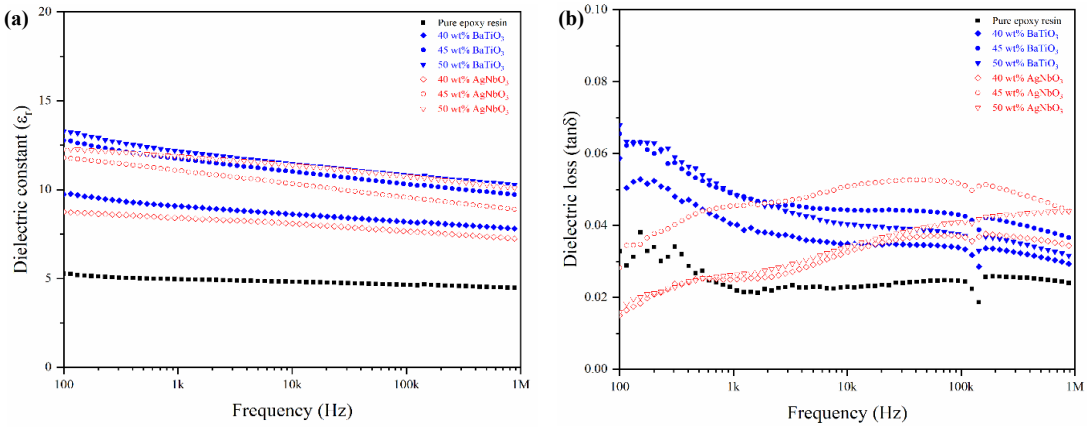


Figure 5. (a) Dielectric constant, and (b) dielectric loss of epoxy resin-based composites filled with ferroelectric $BaTiO_3$ and anti-ferroelectric $AgNbO_3$ particles.

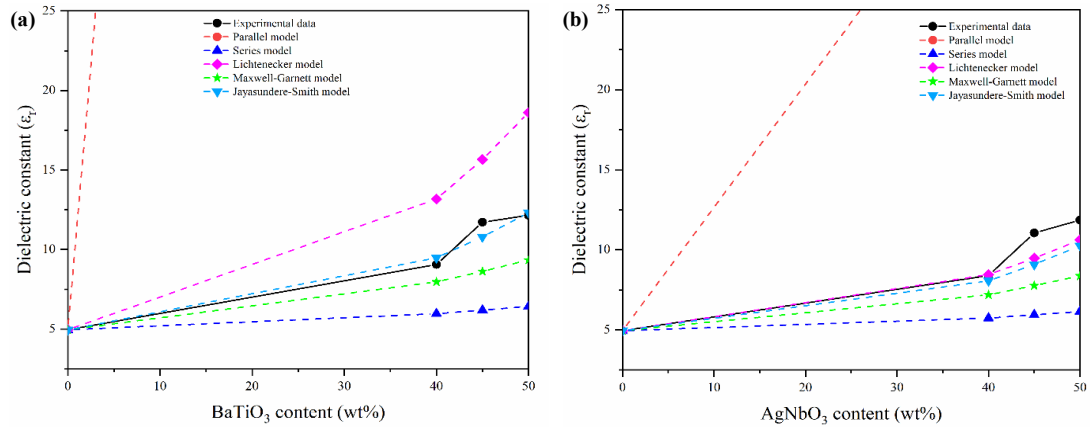


Figure 6. The dielectric constant at 1 kHz for all epoxy resin-based composites filled with (a) ferroelectric $BaTiO_3$, and (b) anti-ferroelectric $AgNbO_3$ particles compared with various theoretical models.

$$\log \varepsilon_C = V_m \log \varepsilon_m + V_f \log \varepsilon_f \quad (2)$$

which assumes homogeneous filler dispersion without considering interfacial polarization or domain effect. The close agreement suggests that the Lichtenecker model provides a reasonable description of the effective dielectric behavior of the $AgNbO_3$/epoxy composites within the investigated filler range. However, the dielectric response may also be influenced by microstructural factors, including particle distribution, aggregation/agglomeration, and polymer-ceramic interfacial characteristics. In contrast, the Jayasundere-Smith model underestimates εr over the investigated filler range.

Despite their different levels of agreement with the dielectric models, the experimental dielectric constants of the $BaTiO_3$/epoxy and $AgNbO_3$/epoxy composites are relatively similar at comparable filler contents. This indicates that the effective dielectric response is not determined solely by the intrinsic dielectric characteristics of the ceramic fillers. The particle size analysis showed broad particle size distributions for both powders, suggesting that particle distribution, agglomeration, and the resulting polymer-ceramic interfacial characteristics may also contribute to the measured dielectric response. The contrasting model performances and dielectric trends should therefore be considered in terms of both the intrinsic dielectric characteristics of the ceramic fillers and their microstructural arrangement within the epoxy matrix. $BaTiO_3$ is a classical ferroelectric material characterized by spontaneous polarization originating from Ti^{4+} ion displacement in its tetragonal lattice. Its intrinsically high dielectric permittivity, together with the dielectric mismatch between $BaTiO_3$ and the epoxy matrix, can contribute to the enhanced dielectric response of the composites. However, as discussed above, microstructural factors such as particle distribution, agglomeration, and polymer-ceramic interfacial characteristics also influence the effective dielectric behavior [2,4,42,43]. In contrast, $AgNbO_3$ exhibits antiferroelectric behavior with anti-parallel dipole ordering in its orthorhombic crystal structure. Although bulk $AgNbO_3$ is known to undergo a field-induced AFE-FE transition at sufficiently high electric fields, the present dielectric and P-E measurements do not provide evidence that such a transition governs the dielectric response of the $AgNbO_3$/epoxy composites. The close agreement with the Lichtenecker model therefore provides an effective description of the experimental dielectric behavior rather than direct evidence of a specific polarization mechanism [8,40]. Overall, the dielectric modelling indicates that the effective dielectric response of the composites results from the combined contributions of intrinsic filler properties, polymer-ceramic interfacial effects, and microstructural characteristics. The different levels of agreement with the theoretical models provide useful descriptions of the dielectric behavior of the two composite systems but should not be regarded as direct evidence of a single dominant polarization mechanism.

3.4 Energy storage performance

The dielectric results discussed above demonstrate that the incorporation of $BaTiO_3$ and $AgNbO_3$ fillers modifies the dielectric response of the epoxy matrix, with the magnitude of the response depending on filler type and content. However, dielectric constant alone does not fully determine the suitability of a material for energy storage applications. A comprehensive evaluation of energy storage performance requires analysis of the polarization-electric field (P-E) hysteresis behavior, which provides insights into polarization switching dynamics, the recoverable energy density, and energy loss under applied electric field. In particular, the recoverable energy density and charge-discharge efficiency derived from P-E loops are critical parameters for assessing the suitability of dielectric materials for capacitive energy storage. Accordingly, the P-E hysteresis loops of $BaTiO_3$/epoxy and $AgNbO_3$/epoxy composites are analyzed in detail in the following section.

Figure 7 presents the P-E hysteresis loops of pure epoxy resin and epoxy-based composites filled with $BaTiO_3$ and $AgNbO_3$ at various filler concentrations. The pure epoxy matrix exhibits a narrow, nearly linear loop with very low polarization, which is characteristic of a predominantly linear dielectric response with limited energy storage capability [17]. The incorporation of either $BaTiO_3$ or $AgNbO_3$ increases the maximum polarization compared with pure epoxy; however, the P-E loops of both composite systems remain relatively slim and quasi-linear within the investigated electric-field range. Moreover, the maximum polarization values of the $BaTiO_3$/epoxy and $AgNbO_3$/epoxy composites are of a similar order of magnitude, indicating that the macroscopic polarization response is not governed solely by the intrinsic ferroelectric or antiferroelectric characteristics of the ceramic fillers [8,44]. For the $BaTiO_3$/epoxy composites, the increased polarization relative to pure epoxy indicates an enhanced dielectric response following

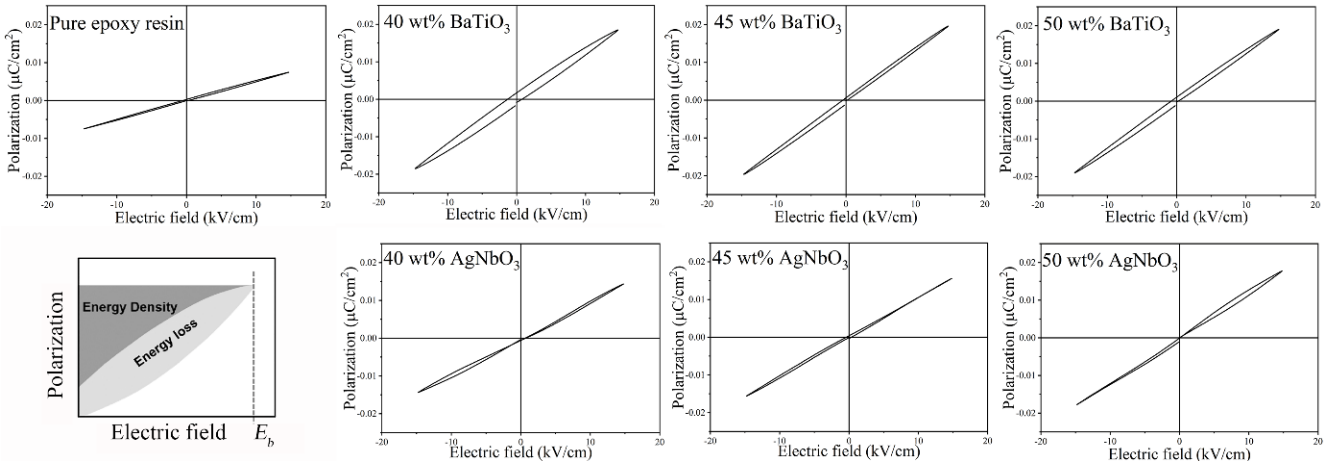


Figure 7. P-E hysteresis loops of $BaTiO_3$/epoxy and $AgNbO_3$/epoxy composites.

incorporation of the high-permittivity ceramic filler. However, a well-developed ferroelectric hysteresis loop is not observed under the present measurement conditions. Similarly, although $AgNbO_3$ is intrinsically antiferroelectric, the P-E loops of the $AgNbO_3$/epoxy composites do not provide sufficiently strong evidence to confirm a field-induced anti-ferroelectric-to-ferroelectric transition. Instead, the relatively slim loops and low remanent polarization indicate a largely reversible polarization response.

To quantitatively evaluate energy storage performance, the recoverable energy density (W_{store}), energy loss density (W_{loss}), and charge-discharge efficiency (η) were calculated from the P-E hysteresis loops using the following relations:

$$W_{store} = \int_0^{P_{max}} EdP \quad (3)$$

$$W_{loss} = \oint EdP \quad (4)$$

$$\eta = \frac{W_{store}}{W_{store} + W_{loss}} \times 100 \quad (5)$$

where Wstore represents the recoverable energy during discharge (area under the right branch of the P-E loop), W_{loss} corresponds to the energy dissipated per cycle (area enclosed by the loop), and η denotes the charge-discharge efficiency. The extracted values P_{max}, P_r, E_c, E_{BD}, W_{store}, W_{loss} and η are summarized in Table 1.

The $BaTiO_3$/epoxy composites exhibit a substantial increase in Wstore with increasing filler content, reaching a maximum value of 134.4 μJ·cm^{-3} at 45 wt%. The enhanced energy-storage capability of the $BaTiO_3$/epoxy composites is associated with the increased polarization response following incorporation of the high-permittivity $BaTiO_3$ filler, together with contributions from polymer-ceramic interfacial polarization and filler-filler interactions. However, these composites also show considerable energy loss (e.g., W_{loss} = 31.9 μJ·cm^{-3} at 45 wt%), resulting in moderate charge-discharge efficiency (η = 78.26%). The higher losses originate from the broader hysteresis loops, internal friction, and interfacial charge trapping. The $AgNbO_3$/epoxy composites exhibit relatively slim P-E loops and low remanent polarization, resulting in reduced hysteresis loss and high charge-discharge efficiency. Although bulk $AgNbO_3$ is known to exhibit field-induced AFE-to-FE transitions, the present P-E measurements do not provide sufficient evidence to attribute the high efficiency of the $AgNbO_3$/epoxy composites directly to such a transition [45]. Instead, the observed high efficiency is primarily associated with their low remanent polarization and highly reversible dielectric response under the investigated electric-field conditions. Notably, both composite systems exhibit comparable dielectric breakdown strengths (E_{BD} ~14.7 kV·cm^{-1} to 14.8 kV·cm^{-1}), confirming that the epoxy matrix retains its structural integrity even at high filler loadings. Overall, these results highlight a clear performance trade-off between the two filler systems: $BaTiO_3$-filled composites provide higher recoverable energy density, whereas $AgNbO_3$-filled composites provide lower energy loss and higher charge-discharge efficiency.

3.5 Hybrid filler composites

To further explore the potential synergy between ferroelectric and antiferroelectric fillers, hybrid $BaTiO_3$-$AgNbO_3$/epoxy composites were fabricated using various mixing ratios while maintaining a constant total filler content of 45 wt%, which was previously identified as the optimum loading for single-filler systems. As summarized in Table 2, the hybrid composites exhibit notable enhancements in both dielectric and energy storage performance compared with the individual $BaTiO_3$-only and $AgNbO_3$-only counterparts. The dielectric constant (ε_r) is highly dependent on the mixing ratio, reaching a maximum value of 13.02 for the 15 wt% $BaTiO_3$/ 30 wt% $AgNbO_3$ hybrid, which exceeds those of both single-filler composites. This enhancement is achieved while maintaining relatively low dielectric loss, suggesting that the incorporation of $AgNbO_3$ contributes to a favorable balance between polarization enhancement and dielectric loss. More importantly, the incorporation of hybrid fillers leads to a substantial improvement in energy storage performance. The recoverable energy density (W_{store}) reaches a maximum value of 155.8 μJ·cm^{-3} for the 15/30 hybrid composition, surpassing those of both $BaTiO_3$-only (134.4 μJ·cm^{-3}) and AgNbO3-only (112.71 μJ·cm^{-3}) composites. In addition, the symmetric 22.5/22.5 mixture exhibits an exceptionally low energy loss of only 1.3 μJ·cm^{-3} and an outstanding charge-discharge efficiency of 99.06%, far exceeding the efficiency of the $BaTiO_3$-only system. These results demonstrate that combining $BaTiO_3$ and $AgNbO_3$ provides complementary dielectric and energy-storage characteristics, in which $BaTiO_3$ contributes to enhanced polarization and energy storage, while $AgNbO_3$ contributes to a more reversible dielectric response and reduced hysteresis loss. Overall, the hybrid filler system successfully integrates the high energy density of $BaTiO_3$ with the high efficiency of $AgNbO_3$, offering a tunable performance profile suitable for next-generation high-efficiency polymer dielectrics and embedded capacitors.

Table 1. Electrical parameters of the epoxy resin-based composites filled with ferroelectric $BaTiO_3$ and anti-ferroelectric $AgNbO_3$ particles, including maximum polarization (P_{max}), remanent polarization (P_r), coercive field (E_c), breakdown strength (E_{BD}), recoverable energy density (W_{store}), energy loss density (W_{loss}) and charge-discharge efficiency (η).

	Pure epoxy resin	$BaTiO_3$/epoxy composites			$AgNbO_3$/epoxy composites		
		40 wt%	45 wt%	50 wt%	40 wt%	45 wt%	50 wt%
P_{max} (μC·cm^{-2})	0.0075	0.0185	0.0196	0.0190	0.0143	0.0156	0.0177
P_r (μC·cm^{-2})	0.0003	0.0017	0.0006	0.0010	0.00005	0.00005	0.00003
E_c (kV·cm^{-1})	0.305	0.842	0.287	0.278	0.673	0.370	0.066
E_{BD} (kV·cm^{-1})	14.68	14.70	14.72	14.72	14.79	14.82	14.79
W_{store} (μJ·cm^{-3})	50.29	114.98	134.4	125.9	108.17	112.71	122.35
W_{loss} (μJ·cm^{-3})	5.66	31.9	12.6	17.6	6.1	3.8	14.4
η (%)	89.88	78.26	91.41	87.75	94.65	96.72	89.48

Table 2. Dielectric properties and energy storage performance of hybrid filler composites.

Filler content [wt%]		Dielectric properties		Energy storage performance		
$BaTiO_3$	$AgNbO_3$	ε_r	$tan\delta$	W_{store} [$\mu J \cdot cm^{-3}$]	W_{loss} [$\mu J \cdot cm^{-3}$]	η [%]
45	0	11.71	0.048	134.4	12.6	91.41
15	30	13.02	0.038	155.8	16.6	90.38
22.5	22.5	11.71	0.036	143.7	1.3	99.06
30	15	12.29	0.039	146.4	16.7	89.76
0	45	11.05	0.045	112.71	3.8	96.72

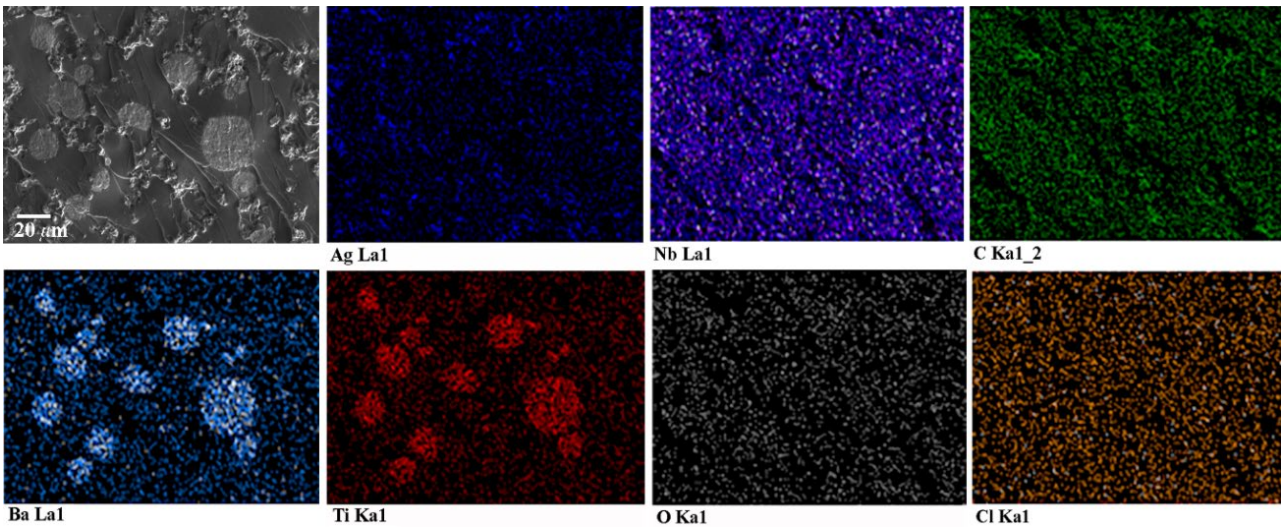


Figure 8. SEM micrograph and EDX elemental mappings of the 15 wt% $BaTiO_3$/30 wt% $AgNbO_3$ hybrid epoxy composite.

To further examine the microstructural characteristics associated with the enhanced performance of the hybrid system, the 15 wt% $BaTiO_3$/30 wt% $AgNbO_3$ composition, which exhibited the highest dielectric constant and recoverable energy density, was selected for SEM and EDX elemental mapping analysis. Figure 8 shows ceramic-rich regions distributed throughout the epoxy matrix, together with some local particle clustering. EDX elemental mapping confirms the coexistence and spatial distribution of Ba and Ti from $BaTiO_3$ and Ag and Nb from $AgNbO_3$ within the analyzed region. These observations demonstrate the incorporation of both ceramic phases within the hybrid composite and the formation of heterogeneous ceramic-polymer and ceramic-ceramic interfacial regions. Such microstructural heterogeneity may contribute to the observed dielectric and energy-storage response through interfacial interactions and local polarization effects.

In summary, the $BaTiO_3$-filled epoxy composites exhibit higher dielectric constants and enhanced polarization, resulting in higher recoverable energy density but moderate efficiency due to greater hysteresis loss. In contrast, the $AgNbO_3$-filled composites exhibit relatively slim P-E loops, low remanent polarization, and high charge-discharge efficiency. The hybrid $BaTiO_3$-$AgNbO_3$ systems combine the complementary dielectric and energy-storage characteristics of both fillers, providing a favorable balance between recoverable energy density and efficiency compared with the corresponding single-filler composites. Notably, the optimal 15/30 hybrid delivers the highest Wstore (155.8 $\mu J \cdot cm^{-3}$), while the 22.5/22.5 hybrid achieves the highest efficiency (99.06%). This combined performance demonstrates the potential of $BaTiO_3$-$AgNbO_3$ hybridization as a strategy for tailoring dielectric and energy-storage properties beyond those obtained using the individual filler systems.

4. Conclusion

Epoxy-based dielectric composites containing ferroelectric $BaTiO_3$ and antiferroelectric $AgNbO_3$ fillers were successfully fabricated and evaluated to investigate their dielectric and energy storage behavior. $BaTiO_3$-filled composites exhibited enhanced dielectric constants and polarization, resulting in increased recoverable energy density, although accompanied by higher hysteresis loss at some compositions. In comparison, $AgNbO_3$-filled composites showed relatively slim P-E loops, low remanent polarization, and high charge-discharge efficiency. Under the electric-field conditions investigated in this study, no conclusive evidence of pronounced ferroelectric switching or a field-induced antiferroelectric-to-ferroelectric transition was observed in the composite systems. By combining these complementary properties, hybrid $BaTiO_3$-$AgNbO_3$/epoxy composites provide an improved balance between recoverable energy density and charge-discharge efficiency, with the optimal 15/30 composition achieving the highest recoverable energy density of 155.8 $\mu J \cdot cm^{-3}$ and the equimolar hybrid reaching an outstanding efficiency of 99.06%. Overall, this study demonstrates that ferroelectric-antiferroelectric hybridization is an effective strategy for simultaneously improving the balance among recoverable energy density, energy loss, and charge-discharge efficiency in epoxy-based dielectrics, offering strong potential for next-generation capacitive energy storage and embedded electronic applications.

Acknowledgement

This work was supported by King Mongkut's Institute of Technology Ladkrabang (KMITL) under Grant No. KREF046706. Apinya Sasipongpan's work was supported under Grant No. KREF016726. Nakulkarn Rerngroen's was supported under Grant No. KREF016724. The authors acknowledge the facilities and technical assistance provided by the Advanced Technology Testing and Analysis Center (ATTAC) of School of Integrated Innovative Technology (SIITec), King Mongkut's Institute of Technology Ladkrabang.

Declaration of competing interest

The authors have no competing interests to declare that are relevant to the content of this article.

References

[1] P. Premwichit, S. Jaila, and S. Prasertpalichat, "Effect of lanthanum doping on phase transition, piezoelectric and energy storage properties of lead-free $0.93(Bi_{0.5}Na_{0.5})TiO_3$-$0.07BaTiO_3$ ceramics," *Journal of Metals, Materials and Minerals*, vol. 35, no. 4, p. e2358, 2025.

[2] S. Priya, and D. J. Inman, *Energy Harvesting Technologies*. New York, NY, USA: Springer, 2009.

[3] Z.-M. Dang, J.-K. Yuan, J.-W. Zha, T. Zhou, S.-T. Li, and G.-H. Hu, "Fundamentals, processes and applications of high-permittivity polymer-matrix composites," *Progress in Materials Science*, vol. 57, pp. 660–723, 2012.

[4] G. H. Haertling, "Ferroelectric ceramics: History and technology," *Journal of the American Ceramic Society*, vol. 82, no. 4, pp. 797-818, 1999.

[5] M. Krupska-Klimczak, S. M. Fathabad, D. Kajewski, R. Sitko, V. V. Shvartsman, D. C. Lupascu, I. Jankowska-Sumara, "Dielectric, piezoelectric, ferroelectric, and electrocaloric properties of Ba, Sr-doped PZT," *Ceramics International*, vol. 51, pp. 19649–19660, 2025,

[6] S. A. Behera, S. Hajra, S. Panda, A. Amanat, and P. G. R. Achary, "Structural and electrical properties of $0.98(K_{0.5}Na_{0.5}NbO_3)$-$0.02(Bi_{0.5}Na_{0.5}TiO_3)$ ceramics," *Journal of Metals, Materials and Minerals*, vol. 33, no. 4, p. 1894, 2023.

[7] G. Liu, S. Zhang, W. Jiang, and W. Cao, "Losses in ferroelectric materials," *Materials Science and Engineering: R: Reports*, vol. 89, pp. 1-48, 2015.

[8] Z. Liu, T. Lu, J. Ye, G. Wang, X. Dong, R. Withers, and Y. Liu, "Antiferroelectrics for energy storage applications: A review," *Advanced Materials Technologies*, vol. 3, p. 1800111, 2018.

[9] H. Moriwake, A. Konishi, T. Ogawa, C. A. J. Fisher, A. Kuwabara, and D. Fu, "The electric field induced ferroelectric phase transition of $AgNbO_3$," *Journal of Applied Physics*, vol. 119, no. 6, p. 064102, 2016.

[10] M. Cao, L. Li, W. B. Hong, S. Y. Wu, and X. M. Chen, "Greatly enhanced permittivity in $BaTiO_3$-epoxy dielectric composites with improved connectivity of ceramic phase," *Journal of Materiomics*, vol. 7, pp. 1–7, 2021.

[11] J. Liu, X. You, N. Chen, and G. Du, "Fabrication of $BaTiO_3$/epoxy composites exhibiting large dielectric constant, low dielectric loss and high flexural strength," *Journal of Wuhan University of Technology-Materials Science Edition*, vol. 34, pp. 1266–1273, 2019.

[12] G. Jian, Y. Jiao, Q. Meng, Z. Wei, J. Zhang, C. Yan, K. -s. Moon, and C. P. Wong "Enhanced dielectric constant and energy density in a $BaTiO_3$/polymer-matrix composite sponge," *Communications Materials*, vol. 1, p. 91, 2020.

[13] H.-Y. Yao, Y.-W. Lin, and T.-H. Chang, "Dielectric properties of $BaTiO_3$-epoxy nanocomposites in the microwave regime," *Polymers*, vol. 13, no. 9, p. 1391, 2021.

[14] M. Z. Khan, F. Aslam, and F. Alsaif, "Enhancing the dielectric characteristics and DC flashover of epoxy resin composites by surface modification of $AgNbO_3$ nanoparticles," *Scientific Reports*, vol. 15, p. 23522, 2025.

[15] K. An, G. Li, T. Fan, F. Huang, W. Wang, and J. Wang, "Enhanced energy storage performance of $AgNbO_3$:xCeO_2 by synergistic strategies of tolerance factor and density regulations," *Coatings*, vol. 13, no. 3, p. 534, 2023.

[16] Z. Wang, T. Zhao, D. Wu, Y. Xue, Z. Yi, J. Kang, R. Ye, and N. Guo, "Enhancing dielectric properties and energy storage performance of polyvinylidene fluoride composite by surface-modified $AgNbO_3$ nanoparticles," *High Voltage*, vol. 9, pp. 939-947, 2024.

[17] L. You, B. Liu, H. Hua, H. Jiang, C. Yin, and F. Wen, "Energy storage performance of polymer-based dielectric composites with two-dimensional fillers," *Nanomaterials*, vol. 13, p. 2842, 2023.

[18] R.Cheng, Y. Wang, R. Men, Z. Lei, J. Song, Y. Li, and M. Guo, "High-energy-density polymer dielectrics via compositional and structural tailoring for electrical energy storage," *iScience*, vol. 25, p. 104837, 2022.

[19] J. Hodgkin, "Thermosets: Epoxies and polyesters," in *Encyclopedia of Materials: Science and Technology*. Elsevier, 2001, pp. 9215–9221.

[20] I. Pasuk, F. Neaţu, S. Neatu, M. Florea, M. C. Istrate, I. Pintilie, and L. Pintilie "Structural details of $BaTiO_3$ nanopowders deduced from the anisotropic XRD peak broadening," *Nanomaterials*, vol. 11, no. 5, p. 1121, 2021.

[21] G. Li, S. Yan, Z. Wang, X. Wang, Z. Li, J. Ye, and Z. Zou, "Synthesis and visible light photocatalytic property of polyhedron-shaped $AgNbO_3$," *Dalton Transactions*, no. 40, pp. 8519–8524, 2009.

[22] H. Liu, X. Wu, Y. Liu, Z. Guo, Q. Ge, and Z. Sun, "The curing characteristics and properties of bisphenol A epoxy resin/maleopimaric acid curing system," *Journal of Materials Research and Technology*, vol. 21, pp. 1655-1665, 2022.

[23] E. Stefan, T. Didriksen, T. O. Sunde, M. L. Fontaine, H. Ræder, and P. M. Rørvik "Effects of powder properties on the 3D printing of $BaTiO_3$ ceramic resins by stereolithography," *Progress in Additive Manufacturing*, vol. 8, pp. 1641-1651, 2023.

[24] M. Sabu, E. Bementa, Y. J. V. Ruban, and S. G. Mon, "A novel analysis of the dielectric properties of hybrid epoxy composites," *Advanced Composites and Hybrid Materials*, vol. 3, pp. 325–335, 2020.

[25] A. Roy, S. Panda, J. Gupta, Anu, R. P. Singh, Deeksha, P. Kour, M. P. Sharma, and K. Yadav, "Effects of interfacial interactions on structural, optical, thermal degradation properties and photocatalytic activity of low-density polyethylene/$BaTiO_3$ nanocomposite," *Polymer*, vol. 276, p. 125932, 2023.

[26] I. A. Asimakopoulos, G. C. Psarras, and L. Zoumpoulakis, "Barium titanate/polyester resin nanocomposites," *Express Polymer Letters*, vol. 8, no. 9, pp. 692–707, 2014.

[27] J.-H. Son, C. A. Ohlin, and W. H. Casey, "Highly soluble iron- and nickel-substituted decaniobates," *Dalton Transactions*, vol. 42, pp. 7529–7533, 2013.

[28] X. S. Xing, and R. K. Y. Li, "Wear behavior of epoxy matrix composites filled with sub-micron silica particles," *Wear*, vol. 256, pp. 21–26, 2004.

[29] Y. R. Uhm, J. Kim, K. J. Son, and C. S. Kim, "Effect of particle size and dispersion on W reinforced polymer composites," *Research on Chemical Intermediates*, vol. 40, pp. 2145–2153, 2014.

[30] M. Samet, A. Kallel, and A. Serghei, "Maxwell-Wagner-Sillars interfacial polarization in composite dielectrics," *Journal of Composite Materials*, vol. 56, no. 20, pp. 3197–3217, 2022.

[31] O. Gulahmadov, L. R. Qahramanli, M. Muradov, N. N. Musayeva, S. Bellucci, and C. Trapalis, "Optimization of MWCNT concentration in polysiloxane nanocomposites for TENGs," *ACS Omega*, vol. 10, no. 42, pp. 50511-50520, 2025.

[32] Z. Wang, R. Ye, D. Wu, Y. Xue, Z. Yi, and Y. Li "Effect of $AgNbO_3$ morphology on dielectric and energy storage properties of polyvinylidene fluoride-based nanocomposites," *ACS Applied Nano Materials*, vol. 6, no. 15, pp. 14374–14382, 2023.

[33] K. Xu, S. Tang, C. Guo, Y. Song, and H. Huang, "Antiferroelectric domain modulation enhancing energy storage performance," *Journal of Materiomics*, vol. 11, p. 100901, 2025.

[34] X. Tang, Z. Zhang, K. Zheng, Y. Wu, Z. Chen, C. Wang, and Z. Shi "Low dielectric loss in poly(vinyl alcohol)/graphene metacomposite films with negative permittivity prepared by spin coating," *Polymer*, vol. 281, p. 126092, 2023.

[35] K. C. Kao, *Dielectric Phenomena in Solids*. Elsevier, 2004.

[36] S. Bronnikov, S. Kostromin, M. Asandulesa, D. Pankin, and A. Podshivalov, "Interfacial polarization in polyazomethine/MWCNTs nanocomposites," *Composites Science and Technology*, vol. 190, p. 108049, 2020.

[37] M. Feng, M. Chen, J. Qiu, M. He, Y. Huang, and J. Lin, "Improving dielectric properties of poly(arylene ether nitrile) composites," *Journal of Alloys and Compounds*, vol. 856, p. 158213, 2021.

[38] H. Wang, and L. Yang, "Dielectric properties and model analysis of electroactive polymers," *Polymer Testing*, vol. 120, p. 107965, 2023.

[39] R. Landauer, "The electrical resistance of binary metallic mixtures," *Journal of Applied Physics*, vol. 23, no. 7, pp. 779–784, 1952.

[40] K. Lichtenecker, and K. Rother, "Die Herleitung des logarithmischen Mischungsgesetzes," *Physikalische Zeitschrift*, vol. 32, pp. 255–260, 1931.

[41] J. C. M. Garnett, "Colours in metal glasses and metallic films," *Philosophical Transactions of the Royal Society of London Series A*, vol. 203, pp. 385–420, 1904.

[42] N. Jayasundere, and B. V. Smith, "Dielectric constant for binary piezoelectric 0-3 composites," *Journal of Applied Physics*, vol. 73, no. 5, pp. 2462–2466, 1993.

[43] A. Bouhamed, S. Missaoui, A. B. Ayed, A. Attaoui, D. Missaoui, K. Jeder, N. Guesmi, A. Njeh, H. Khemakhem, and O. Kanoun, "A comprehensive review of strategies toward efficient flexible piezoelectric polymer composites based on $BaTiO_3$ for next-generation energy harvesting," *Energies*, vol. 17, p. 4066, 2024.

[44] J. Zhou, Z. Xu, H. Yang, L. Chu, L. Chen, H. Li, J. Ding, S. Ran, Z. Sun, and X. Hao, "Excellent energy storage performance of lead-based antiferroelectric ceramics via enhancing dielectric breakdown mechanism," *Chemical Engineering Journal*, vol. 487, p. 150476, 2024.